Relevance of non-exponential single-defect-induced threshold voltage shifts for NBTI Variability

Jacopo Franco*, Ben Kaczer, Philippe J. Roussel, Maria Toledano-Luque, Pieter Weckx
imec
Leuven, Belgium
*Jacopo.Franco@imec.be

Tibor Grasser

Technische Universität Wien,
Wien, Austria

***Abstract*—We report statistical NBTI datasets of nanoscale Si/SiON pMOSFETs. Weibull-distributed single-defect-induced ΔV_{th} are observed in the NBTI relaxation transients, in contrast with literature reports of exponential distribution. We discuss the (ir)relevance of a correct description of the single-defect-induced ΔV_{th} steps for describing the total BTI induced ΔV_{th} distribution. We show that the BTI induced V_{th} variance can be correctly predicted based on time-zero V_{th0}-variability only.**

Keywords—NBTI, pMOSFETs, Variability.

I. Introduction

Due to the ever decreasing device dimensions, the number of dopant atoms, as well as the number of defects in each device is being reduced to a enumerable level [1]. This results in intrinsic time-zero V_{th0}-variability, but also considerable time-dependent variability. Each nominally identical nanoscale transistor shows a different V_{th}-shift after identical BTI stress. Hence the deterministic degradation curve and time-to-failure measured on large area devices need to be replaced by distributions [2,3].

A correct description of the BTI induced variability is crucial for robust circuit design, in order to ensure circuit functionality at product end of life by including sufficient margins for the V_{th0}-variability, the median V_{th} shift, and the additional V_{th}-variance induced by BTI. The BTI induced ΔV_{th} distribution has been recently described as the convolution of a Poisson-distributed number of charged defects per device, with exponentially distributed single-defect-induced ΔV_{th}*'s* [4].

In this paper we report NBTI datasets measured on lowly-doped nanoscale Si/SiON pMOSFETs. Weibull-distributed single-defect-induced ΔV_{th} are observed in the NBTI relaxation transients. We extend the previously proposed model of BTI variability to a convolution of Poisson and Weibull distributions, and we discuss the (ir)relevance of a correct description of the single-defect ΔV_{th} distribution. We show that, for a given median V_{th}-shift, the additional V_{th} variance induced by BTI can be correctly predicted based on V_{th0} variability only; therefore, circuit design margin for BTI variability can be directly derived from the typically available info about the V_{th0} variability of the considered technology. This finding lowers the importance of an accurate description of the distribution of single-defect-induced V_{th} shifts in a given technology, which would typically require a significant experimental effort.

II. Experimental

NBTI measurements [4] were performed on nanoscale Si/SiON pMOSFETs, with channel width and metallurgical length of 90 and 35 nm respectively, and a capacitance equivalent thickness of ~2.75 nm. Each device was stressed for 100 s at a gate overdrive voltage of -1.6 V. Subsequently NBTI relaxation was monitored from 1 ms up to 1000 s in order to observe the emission of single holes trapped in oxide defects during the stress phase and to obtain the ΔV_{th} distribution as a function of the relaxation time, i.e. including the impact of a varying number of charged defects.

III. Results and discussion

Fig. 1 shows the V_{th0} distribution measured on fresh devices at room temperature and at 125°C. Normal-distributed V_{th0} are observed, with standard deviation σ_{Vth0} ~23.4 mV. We have previously observed [5,6] that the average single-defect-induced ΔV_{th} ($\equiv\eta$), which determines the BTI induced V_{th} variance, can be roughly derived from V_{th0} variability since the two phenomena are related to the same root cause–the percolative nature of current flow in nanoscale devices mainly due to Random Dopant Fluctuation [1]. The variance of the BTI V_{th} shift in a device population can be expressed as [7]

$$\sigma^2_{\Delta Vth} = 2\eta\langle\Delta V_{th}\rangle. \quad (1)$$

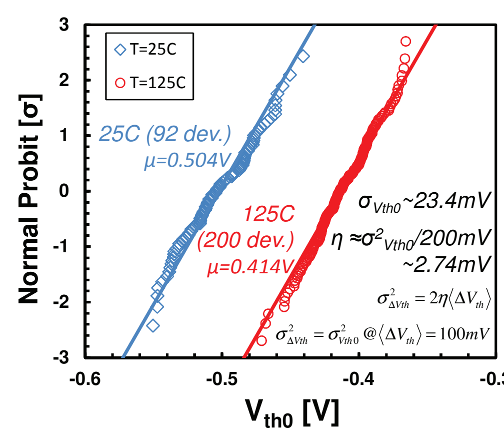

Figure 1: Measured initial threshold voltage distributions, for T=25°C and 125°C. The estimated V_{th0} standard deviation (σ_{Vth0}) is ~23.4mV, which projects to an average impact per single charged defect $\eta\approx\sigma^2_{Vth0}/0.2V$=2.74mV, cf. Eqs. (1-2).

978-1-4799-0352-8/13/$31.00 ©2013 IEEE

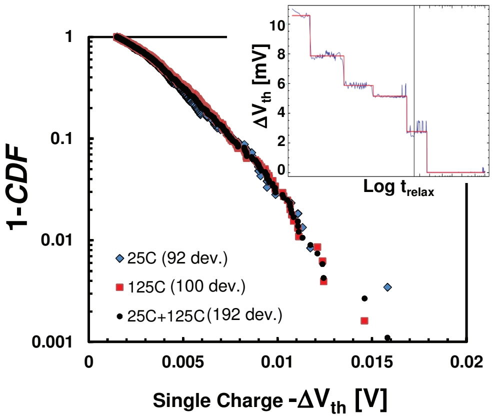

Figure 2: Complementary CDF of the single-charge-induced ΔV_{th} experimentally observed on 92 devices at room temperature, and on other 100 devices at 125°C. The same distribution is observed, with a total of 635 hole emission events observed in the 192 devices. The plot was constructed by collecting the discrete ΔV_{th} steps observed in the NBTI relaxation transients (inset).

In [6], by comparing experimental data from different technologies, we have observed that the variance of the BTI induced ΔV_{th} distribution equals the V_{th0} variance when the median BTI shift is $\langle\Delta V_{th}\rangle\approx$100mV. We can therefore express η as a function of the initial V_{th0} variability as:

$$\eta = \frac{\sigma^2_{\Delta Vth}}{2\langle\Delta V_{th}\rangle} = \frac{\sigma^2_{Vth0}}{200mV}. \qquad (2)$$

From the experimental V_{th0} distribution shown in Fig. 1 we can estimate an average single-defect-induced shift $\eta \approx$2.74 mV. We note that this η value is comparable to the charge sheet approximation for a single charge ($=q/C_{ox}$), while typically larger η values have been reported [4-6], possibly due to different channel doping profiles. In the following we compare the predicted BTI induced ΔV_{th} distribution based on this estimate from V_{th0} variability and based on an accurate characterization of the single-defect-induce impacts at the single device level.

Fig. 2 shows the experimental distribution of single-defect-induced ΔV_{th}'s observed as discrete steps in the NBTI relaxation transients (inset). Each device shows a different number of charging/discharging defects, with average value $\langle N_T\rangle$, and each charged defect causes a different ΔV_{th} impact, with median value η [4]. While more defects are charged at elevated temperature, the same distribution of individual defect impacts is observed in the device stressed at 25°C and 125°C, suggesting a negligible effect of the temperature on the percolation path configuration in the channel [8].

Typically the single charge ΔV_{th}'s have been observed to follow an exponential distribution with median value η: a Maximum Likelihood fit to the data yielded the best estimate η ~2.9 mV [Fig. 3 (a)]. Note that this value is very close to the estimate based on the V_{th0} distribution [see Eq. (2)]. However, a significant deviation from the exponential model is observed at low percentiles. In contrast, a Weibull distribution with η ~4.12 mV and β ~1.51 was found to describe significantly better the experimentally observed single-defect ΔV_{th} [Fig. 3 (b) and (c)] down to low percentiles.

Fig. 4 shows the ΔV_{th} distribution measured on 92 devices (±2.5σ), as a function of the relaxation time (1 ms → 1000 s). Note the ΔV_{th} measured on each device is due to the cumulative effect of a varying number (*zero* or more) of charging defects. For increasing relaxation times, hole emission events from the defect sites reduce the average number of defects remaining charged (i.e., $\langle N_T\rangle$ depends on the considered relaxation time).

In [4] we have shown that the number of charged defects per device is Poisson distributed, with the probability mass function (PMF) being

$$PMF = \frac{\langle N_T\rangle^{N_i}}{N_i!}\exp\left(-\langle N_T\rangle\right), \qquad (3)$$

where N_i is the actual number of charged defects in each device. Each charged defect cause a different ΔV_{th}, described by the Cumulative Density Function (CDF):

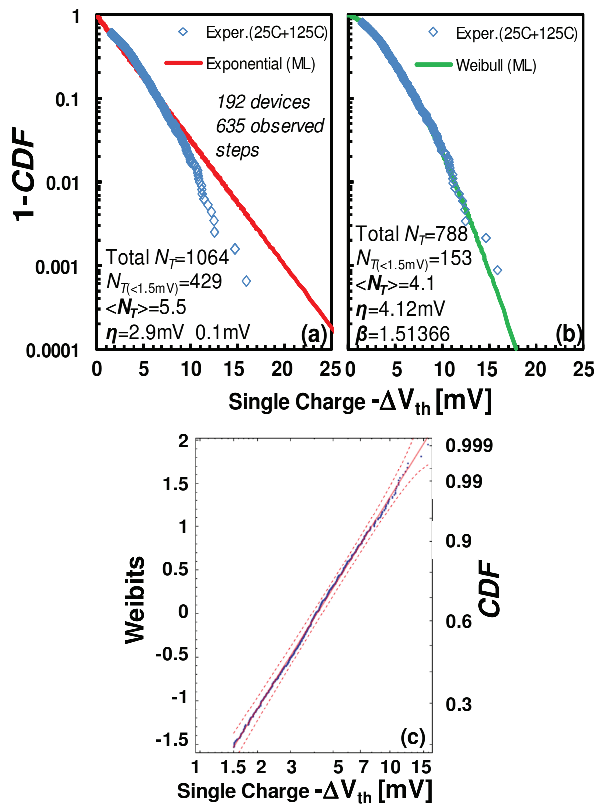

Figure 3: **(a)** Complementary CDF of the observed single charge induced ΔV_{th} (25°C and 125°C) fitted with a Maximum Likelihood procedure to an exponential distribution. The fit yields η ~2.9 mV, and an average number of charged defects per device $\langle N_T\rangle$ ~5.5. However a significant deviation of the experimental data is observed at low percentiles. **(b)** and **(c)** A significantly better description of the experimental data is obtained with a Weibull distribution. In this case the fitted parameter are η ~4.1 mV, β ~1.51, and $\langle N_T\rangle$ ~4.1.

$$CDF: 1 - \exp\left(-\frac{\Delta V_{th\_i}}{\eta}\right)^{\beta}, \qquad (4)$$

with β=1 for an exponential distribution. To describe the experimental ΔV_{th} we used a Monte Carlo approach to compute the convolution of the Poisson distributed number of defects [Eq. (3)], with exponential- or Weibull-distributed impacts [Eq. (4)]. The simple Monte Carlo loop is schematically depicted in Fig. 5.

The experimental data appear equivalently well described by using either exponential- [Fig. 4 (a)] or Weibull-distributed ΔV_{th} impacts [Fig. 4 (b)], with η and β parameters obtained from the Maximum Likelihood fits to the measured distribution of single-defect impact of Fig. 3. Note the $\langle N_T \rangle$ parameter was fitted in order to match the experimentally observed median shift $\langle \Delta V_{th} \rangle$; for the approach based on the exponential distribution the fitted value of $\langle N_T \rangle$ was equal to $\langle \Delta V_{th} \rangle / \eta$, as derived in [7].

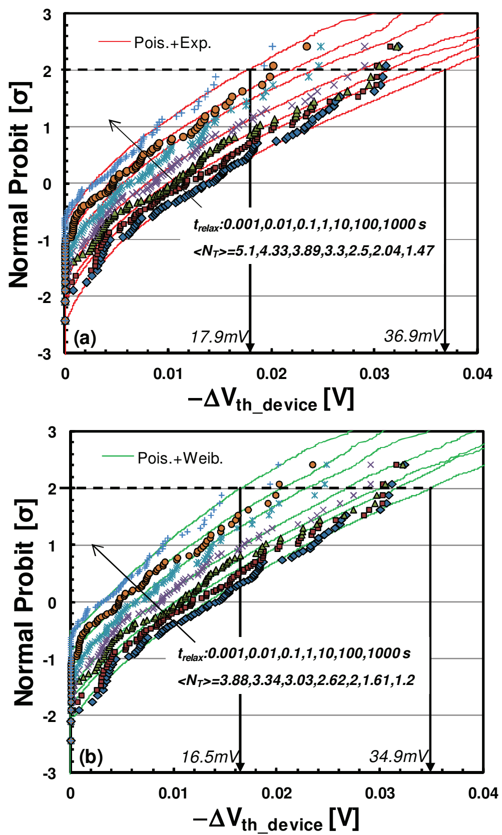

Figure 4: Measured ΔV_{th} distribution after 100 s of NBTI stress at V_{ov}=$V_{Gstress}$-V_{th0}= -1.6 V, T=25°C, for increasing relaxation times (1 ms→1000 s). **(a)** The experimental data are well described by a convolution of Poisson-distributed number of charge defects with exponentially distributed impacts (η=2.9mV). The average number of defects $\langle N_T \rangle$ was obtained as $\langle \Delta V_{th} \rangle / \eta$ [4]. Note the decreasing $\langle N_T \rangle$ for increasing relaxation times due to hole emission. **(b)** The same data are equally well described by using a Weibull-distributed impact per defect (η~4.1mV, β~1.51). Note the ~22% lower $\langle N_T \rangle$ and the only slightly lower ΔV_{th} at high percentiles (2σ values are demarcated by the arrows).

```
for i=1:1:N_devices
   N_i=random('Poisson', ⟨N_T⟩);
   ΔV_th_dev=0
   for j=1:1:N_i
      ΔV_th_dev += random('Weibull', η, β);
   end
end
```

Figure 5: Schematic representation of the simple Monte Carlo loop implemented to calculate the distribution of ΔV_{th} in a device population, based on the Poisson distribution of charged defects per device, with exponential- or Weibull-distributed impacts (note: β=1 for the exponential distribution).

To compare the two approaches ('Poisson+exponential' vs. 'Poisson+Weibull'), we computed the expected ΔV_{th} distribution for increasing $\langle \Delta V_{th} \rangle$ up to ~100mV, i.e. up to product end of life (Fig. 6). No significant difference in the ΔV_{th} variance predicted by the two approaches is observed up to ±3σ. We note that the approach based on the Weibull distribution seems to predict a slightly narrower ΔV_{th} distribution beyond 3σ. However, an analytic formulation of the convolution of Poisson and Weibull distributions would be needed to accurately compare the two predictions at higher percentiles of relevance for, e.g., SRAM applications [9] (note: the analytic formulation of the convolution of Poisson and Exponential distributions was derived in [7]).

Furthermore we found that a ΔV_{th} distribution computed as the convolution of Poisson and exponential with η directly derived from V_{th0} variability [see Eq. (2)], also describes the NBTI induced variance sufficiently well (Fig. 6, dashed line). This finding lowers the importance of an accurate description of the distribution of single-defect-induced V_{th} shifts at very low percentiles, which typically requires a significant experimental effort.

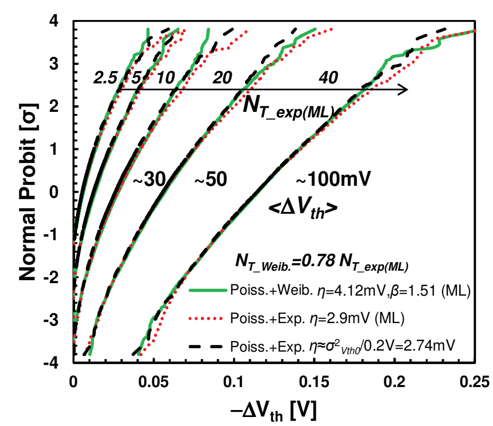

Figure 6: ΔV_{th} distribution computed with the Monte Carlo approach by convoluting a Poisson distribution of charged defect per device, with the Weibull (solid) or exponential (dotted) distribution of single-defect-induced ΔV_{th}. No significant difference is observed up to ±3σ. Note that in order to yield the same median $\langle \Delta V_{th} \rangle$ value, a ~22% reduced average number of defect per device $\langle N_T \rangle$ has been used in the former case (since $\eta_{Weib.} > \eta_{Exp.}$). The computed distribution based on Poisson+exponential, with η derived from V_{th0} variability (dashed) is shown to predict the NBTI induced variance and to match the other descriptions sufficiently well.

In Fig. 7 the measured ΔV_{th} distribution after NBTI stress at T=25°C and 125°C (fixed overdrive voltage and stress time) are compared. The high temperature stress induced larger $\langle\Delta V_{th}\rangle$ due to increased average number of charged defects $\langle N_T\rangle$. Notice that the typical BTI dependences on stress voltage, stress time and temperature can be included in $\langle N_T\rangle$ as we discussed in [10], e.g. as:

$$\langle N_T\rangle \propto \exp\left(\frac{-E_A}{k_B T}\right)\left(\frac{V_G - V_{th0}}{t_{ox}}\right)^{\gamma} t^{n}_{stress}, \qquad (5)$$

where E_A is the activation energy (typical apparent value for NBTI ~60 meV), γ is the voltage acceleration (typical NBTI value ~3 in Si devices), and n is the time exponent (typical apparent value ~0.15). The measured distributions for the stress at room temperature and at elevated temperature are well described by the model independently of the used description of the single-defect ΔV_{th}, by simply adjusting the parameter $\langle N_T\rangle$ in order to match the observed $\langle\Delta V_{th}\rangle$ (see Fig. 7 inset).

We conclude that the V_{th} distribution after a BTI stress inducing a given $\langle\Delta V_{th}\rangle$ can be well predicted based on V_{th0} variability only, as shown in Fig. 8. Therefore, design margin to cope with the BTI induced variability can be evaluated at an early design stage, based on the V_{th0} variability information which is typically available to circuit designers for the used technology.

IV. Conclusions

We have reported NBTI datasets of nanoscale Si/SiON pMOSFETs. Weibull-distributed single-defect ΔV_{th} were observed in the NBTI relaxation transients, in contrast with typical reports of exponential distribution. We have discussed the (ir)relevance of an accurate description of the single-defect ΔV_{th} to correctly describe the total BTI ΔV_{th} distribution. While differences might arise in the tails of the total ΔV_{th} distribution, these tails are typically experimentally inaccessible, and the experimental data (which represents mainly the bulk of the distribution) can be well described irrespectively of the assumed single-defect ΔV_{th} distribution. Finally we have confirmed that the BTI induced V_{th} variance can be directly derived from V_{th0} variability only. This finding allows circuit designers to include margins for BTI induced variability based on the typically available information about the V_{th0} variability of the used technology.

Acknowledgment

This work was performed as part of imec's Core Partner Program. It has been in part supported by the European Commission under the 7th Framework Programme (Collaborative project MORDRED, contract No. 261868).

References

[1] A. Asenov, R. Balasubramaniam, A. R. Brown, and J. H. Davies, "RTS Amplitude in Decananometer MOSFETs: 3-D Simulation Study", in *IEEE* Trans. Electron Devices, Vol. 50, no. 3, pp. 839-845, 2003;

[2] T. Grasser *et al.*, "Recent Advances in Understanding the Bias Temperature Instability", in *IEEE Proc.* International Electron Device Meeting (IEDM), pp. 82-85, 2010;

[3] A. Kerber and T. Nigam, "Challenges in the characterization and modeling of BTI induced variability in metal gate / High-k CMOS technologies", in *Proc. IEEE* International Reliability Physics Symposium (IRPS), pp. 2D.4.1-6, 2013;

[4] B. Kaczer *et al.*, "Origin of NBTI Variability in Deeply Scaled pFETs", in *Proc. IEEE* International Reliability Physics Symposium (IRPS), pp. 26-32, 2010;

[5] J. Franco *et al.*, "Reduction of the BTI Time-Dependent Variability in Nanoscaled MOSFETs by Body Bias", in *IEEE Proc.* International Reliability Physics Symposium (IRPS), pp. 2D.3.1-6, 2013;

[6] M. Toledano-Luque *et al.*, "Degradation of time dependent variability due to interface state generation", in *Proc.* Symp. VLSI Tech., pp. T190-191, 2013;

[7] B. Kaczer, Ph.J. Roussel, T. Grasser, and G. Groeseneken, "Statistics of Multiple Trapped Charges in the Gate Oxide of Deeply Scaled MOSFET Devices—Application to NBTI", in *IEEE* Electron Device Letters, Vol. 31, no. 5, pp. 411-413, 2010;

[8] M. Toledano-Luque *et al.*, "From Mean Values to Distributions of BTI Lifetime of Deeply Scaled FETs through Atomistic Understanding of the Degradation", in *Proc.* Symp. VLSI Tech., pp. T152-153, 2011;

[9] P. Weckx *et al.*, "Implications of BTI induced time-dependent statistics on yield estimation of digital circuit", submitted;

[10] J. Franco *et al.*, "SiGe Channel Technology: Superior Reliability toward Ultra-Thin EOT devices–Part II: Time-Dependent Variability in Nanoscaled Devices and Other Reliability Issues", *IEEE* Trans. Electron Devices, Vol. 60, no. 1, pp. 405-412, 2013.

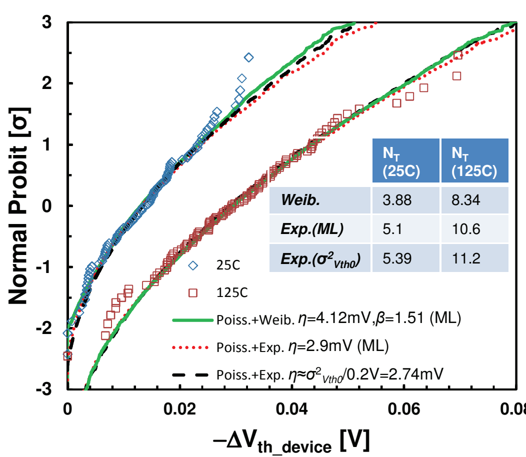

Figure 7: Measured ΔV_{th} distribution after 100s of NBTI stress at V_{ov}=-1.6 V, t_{relax}=1 ms, T=25°C or 125°C. A good description of the spread of the experimental data is obtained independently of the used description of the single-defect-induced ΔV_{th}: Weibull (solid) or Exponential (dotted) distributions with parameters obtained by fitting experimental single defect ΔV_{th}, or Exponential (dashed) with η derived from V_{th0} variability ($\eta \approx \sigma^2_{Vth0}$/0.2V). The inset reports the fitted $\langle N_T\rangle$ values.

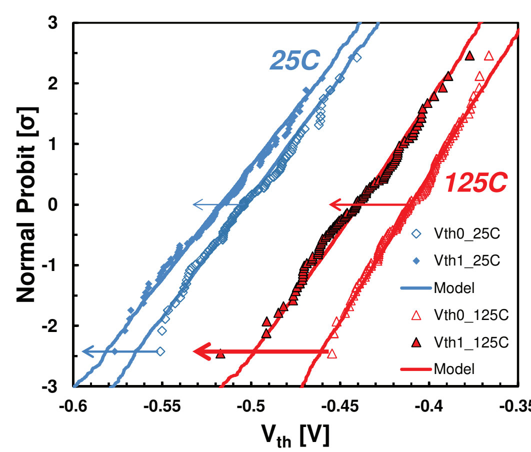

Figure 8: Measured V_{th} distribution in fresh devices (open) and after NBTI stress (solid, t_{relax}=1ms), at T=25°C (diamonds) or 125°C (triangles). Notice that NBTI induces both an average V_{th}-shift and an additional V_{th}-variability. The V_{th} distribution after NBTI stress are well described by the model we proposed in [4], based on the convolution of Poisson-distributed charged defect per device causing exponentially distributed ΔV_{th} steps, with average value $\eta \approx \sigma^2_{Vth0}$/0.2V.